Research Journal of Applied Sciences, Engineering and Technology 11(3): 252-258, 2015
DOI: 10.19026/rjaset.11.1714
ISSN: 2040-7459; e-ISSN: 2040-7467

Submitted: October 22, 2014 Accepted: December 18, 2014 Published: September 25, 2015

Research Article

Evaluation of Residual Stresses in Low, Medium and High Speed Milling

[1]F.V. Díaz, [1]C.A. Mammana and [2]A.P.M. Guidobono
[1]Departamento de Ingeniería Electromecánica-Departamento de Ingeniería Industrial, Facultad Regional Rafaela, Universidad Tecnológica Nacional, Acuña 49, 2300 Rafaela, Argentina
[2]División Metrología Dimensional, Centro Regional Rosario (INTI), Ocampo y Esmeralda, 2000 Rosario, Argentina

Abstract: A micro-indent method is used to evaluate different residual stress states, which were generated in samples of AA 7075-T6 aluminium alloy milled at low, medium and high speed. The milling tests were carried out in order to introduce, in each new surface, two different zones from asymmetries in the orientation of the cutting edge. The results obtained in samples subjected to different combinations of process parameters reveal, in both cutting zones, compressive normal components regardless of the evaluated direction. This study includes a comprehensive analysis of the medium normal component of residual stress. This component is the most representative of the stress tensor since it is independent of the diameter of the stress circle, commonly denominated Mohr's circle. In addition, this component is associated to those directions where tangential components reach their maximum. From the sensitivity of the used method, it was possible to detect differences generated between the levels reached by the medium component in the evaluated zones. It is noteworthy that the detected differences are independent of the cutting speed and feed rate. This significant fact, finally, would indicate similar differences in the combination of local plastic deformation and heat conducted to the new surface between both cutting zones, which is valid for different combinations of process parameters evaluated in this study.

Keywords: Aluminium alloy, indent method, milling, mohr's circle, residual stresses

INTRODUCTION

All machining processes performed in the industry field generate residual stresses (Brinksmeier *et al*., 1982). These stresses are very important because they can produce adverse effects in a machined component both in terms of geometry and in terms of service life (Schwach and Guo, 2006; Withers, 2007). Although, over the years, diverse studies have been conducted in the field of residual stresses induced by machining (Henriksen, 1951; Brinksmeier, 1987; Fuh and Wu, 1995; Capello, 2005; Abrão *et al*., 2011), the structural mechanisms that generate these stresses are not entirely comprehended because of the complexity in the combination of mechanical and thermal effects associated to such generation.

In face milling, the instantaneous orientation of the cutting edge changes regarding a reference system fixed in the milled surface (Jacobus *et al*., 2001). This change implies that the chip formation process and the associated plastic deformation will instantly change in orientation. Because of this fact, it is expected that the levels of residual stresses accompany these instantaneous changes. Furthermore, the chip thickness changes continuously, generating instantaneous changes regarding the heat flow from the primary deformation zone to the generated new surface (Özel and Zeren, 2004). Thus the temperature of this surface will continuously change due to the cutting edge movement, affecting the generation of residual stresses.

The purpose of this study is to delimit two zones, in the surfaces introduced via face milling, generated from asymmetries in the orientation of the cutting edge, in order to conduct a thorough analysis of the similarities and differences of normal and tangential components of residual stress in these zones. It is noteworthy that, in most of the studies published to date, the analyses do not take into account variations that occur in the residual stresses due to the cutting edge path performed in the different zones. These variations would play an important role both in geometric distortion and in service life of different milled components. In this study, a method of micro-indents (Wyatt and Berry, 2006) was used to determine normal and tangential components of residual stress. Different tests of low, medium and high speed were performed in samples of AA 7075-T6 aluminium alloy. These tests were carried out using a vertical machining

Corresponding Author: F.V. Díaz, Departamento de Ingeniería Electromecánica-Departamento de Ingeniería Industrial, Facultad Regional Rafaela, Universidad Tecnológica Nacional, Acuña 49, 2300 Rafaela, Argentina, Tel.: +54 3492 432710; Fax: +54 3492 422880

center numerically controlled. The feed rate was varied to assess the effects generated in the different components of residual stress. Finally, one of these components, the medium normal, which was not researched in previous studies on the field, allowed identifying that the plastic stretching difference between both evaluated zones would be the same for different combinations of cutting speed and feed rate. This fact indicates that the combination of local plastic deformation (mechanical effect) and heat conducted to the new surface (thermal effect) would also present the same differences between the evaluated cutting zones.

EXPERIMENTAL PROCEDURE

As mentioned above, in this study different face milling tests were carried out to determine the main similarities and differences regarding residual stresses generated in asymmetrical and adjacent zones. These stresses were determined at different points of each generated surface. Figure 1 shows the milled surface (63×40 mm) and the location of those points (A and B), which are the centroids of the zones. These zones may be denominated as conventional (x>0, y) and climb (x<0, y) cutting zones. The face milling tests were performed using a numerically controlled vertical machining center (Victor Vc-55) installed in a laboratory. This machining center uses a self-balanced face mill of 63 mm in diameter. This face mill has five circumferentially spaced inserts (Palbit SEHT 1204 AFFN-AL SM10) of tungsten carbide. It is important to mention that these inserts have been specially designed for milling high strength aluminium alloys (Díaz *et al*., 2010). Table 1 shows the different combinations of process parameters for each of the performed tests. It is noteworthy that the same depth of cut was selected for all tests.

These tests were carried out in samples prepared from a rolled product of AA 7075-T6 aluminium alloy 4 mm thick. Table 2 and 3 give the chemical composition and mechanical characteristics of the rolled product, respectively. The optical microscopy revealed a grain structure of solid solution α (Al). The grains, elongated in the rolling direction (GS: 40×8 μm), show fine precipitated particles of (Fe, Mn)Al_6 and $CuMgAl_2$ aligned in that direction. The micro-hardness of this material was assessed at different points; the mean value obtained was 186 HV0.5.

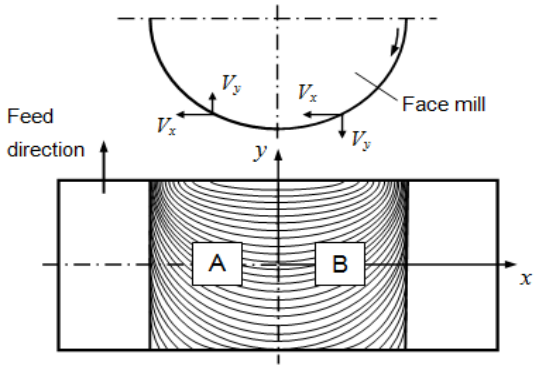

Fig. 1: Milled surface

The aforementioned tests were performed in samples free of residual stresses. The heat treatment to relieve these stresses was conducted after preparing the geometry of the samples (110×40×4 mm). Regarding the values corresponding to that treatment, they were 300°C and 80 min. Finally, the cooling process was carried out in the furnace (Dalvo HM2).

Regarding the implementation of the micro-indent method used in the present work, all details can be consulted in previous studies (Díaz *et al*., 2010; Díaz and Mammana, 2012). Concisely, this method consists in introducing a series of micro-indents in the milled surface. Then, before and after a thermal relaxation treatment, the micro-indent coordinates are measured using a universal measuring machine of high precision (Curtis and Farago, 1994). It is noteworthy that this machine is very versatile which allows carrying out

Table 1: Selected process parameters

	Process parameters			
Test number	Cutting speed V (m/min)	Feed per tooth f_z (mm/tooth)	Table feed v_f (m/min)	Depth of cut d (mm)
1	100	0.08	0.20	0.40
2	100	0.16	0.40	0.40
3	300	0.08	0.60	0.40
4	300	0.16	1.20	0.40
5	1000	0.08	2.00	0.40
6	1000	0.16	4.00	0.40

Table 2: Chemical composition (wt %) of the investigated aluminium alloy

Zn	Mg	Cu	Fe	Si	Cr	Mn	Al
5.6	2.52	1.72	0.32	0.2	0.17	0.16	Balance

Table 3: Mechanical properties of the investigated aluminium alloy

Properties				
σ_u (MPa)	$\sigma_{y_{02}}$ (MPa)	A (%)	E (GPa)	v
564	506	11	70	0.33

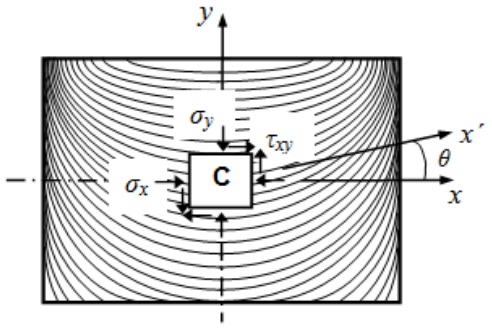

Fig. 2: Residual stress components in the centroid C

different types of measurements in mechanical components, including the determination of orthogonal coordinates (x, y, z) at any point. This determination is possible through the use of a high resolution micrometer microscope (Dotson *et al*., 2003), which is assembled in the main header of the machine.

Figure 2 shows the residual stress state in the centroid of the generated surface (point C). For obtaining the different residual stress components at any point of the new surface, four micro-indents must be introduced. Each of these will correspond to a vertex of an imaginary square whose centroid is the point to evaluate (Díaz and Mammana, 2012). In this study, the micro-indents were introduced using a Vickers micro hardness tester (Shimadzu HMV-2). As previously mentioned, after the introduction of these micro-indents it is possible to measure, before and after a thermal relaxation treatment (300°C and 80 min), the micro-indent coordinates using a measuring machine (GSIP MU- 314). It should be noted that if the relaxation treatment is performed below the recrystallization temperature (Mao, 2003), the dimensional changes at the specimen will be governed only by the elastic relaxation of the lattice (the plastic flow activated by temperature is highly localized and it can be reduced to the annihilation of vacancies and dislocations of opposite sign and to the rearrangement of dislocations into lower-energy configurations). In addition, if the specimen geometry is simple, the thickness is small and the cooling rate is slow, it is possible to avoid the development of thermal residual stresses.

Then, through the processing of the measured coordinates (Mammana *et al*., 2010), it is possible to obtain the components of residual strain ε_x, ε_y and γ_{xy}, which correspond to the centroid of the square. From these components and assuming that the evaluated surface is under plane stress conditions (Gere, 2001), the components of residual stress in the case of a linear elastic, homogeneous and isotropic material, can be expressed as:

$$\sigma_{x'} = \frac{\sigma_x + \sigma_y}{2} + \frac{\sigma_x - \sigma_y}{2}\cos 2\theta + \tau_{xy} \cdot \sin 2\theta \qquad (1)$$

$$\tau_{x'y'} = -\frac{\sigma_x - \sigma_y}{2}\sin 2\theta + \tau_{xy} \cdot \cos 2\theta \qquad (2)$$

where, σ_x, σ_y and τ_{xy}, obtained from ε_x, ε_y and γ_{xy}, are the components of residual stress corresponding to the original reference system and θ is the angle associated to the direction of evaluation with respect to the reference axis x (Fig. 2).

Finally, the measurement error corresponding to the present method was estimated in the range of ±0.9 MPa (Díaz *et al*., 2010). It is important to note that the micro-indents coordinates were measured within a temperature range of 20±0.2°C, with a rate lower than 0.01°C/min. It is noteworthy that if this rate is higher than that value, the measurement error will increase significantly.

RESULTS AND DISCUSSION

Figure 3 shows different normal components of residual stress, which were evaluated as functions of cutting speed. Each function corresponds to a centroid, a value of feed rate and a value of depth of cut, which is the same for all cases (d = 0.4 mm). The most important feature of these functions is that they are negative and decreasing. In Fig. 3a the σ_x component is shown. It is remarkable that the abscissa values are expressed in logarithmic scale. From this scale three functions are linear or quasi-linear. On the one hand, for V = 100 m/min, the obtained values show some dispersion. For this low cutting speed, the feed rate f_z = 0.16 mm/tooth would be too high causing a plastic stretching larger than expected in the conventional cutting zone. On the other hand, for V = 300 m/min and V = 1000 m/min, the values for both centroids coincide when both feed rates are evaluated separately. This is because the component V_x of cutting speed has the same module and direction in both centroids and, simultaneously, it is perpendicular to feed direction (Fig. 1). Moreover, given that the segments between V = 300 m/min to V = 1000 m/min are parallel, the increments of σ_x from the cutting speed change will be similar regardless of the evaluated centroid and feed rate. From this fact, it could be inferred that the plastic stretching difference when cutting speed is increased 700 m/min is the same for each of the combinations of centroids and feed rates.

Figure 3b shows the σ_y component. In contrast with the σ_x component, in this case the functions become more compressive from the centroid A to B, for each of the feed rates. This is due to that, at the point A, the cutting speed component V_y and feed rate have the same direction and, at the point B, both have opposite directions (Fig. 1). The functions are linear and parallel for the lower feed rate. However, for the higher feed rate, the functions can be considered only quasi-parallel in each of the segments. For V = 100 m/min, the values obtained at each centroid are independent of the

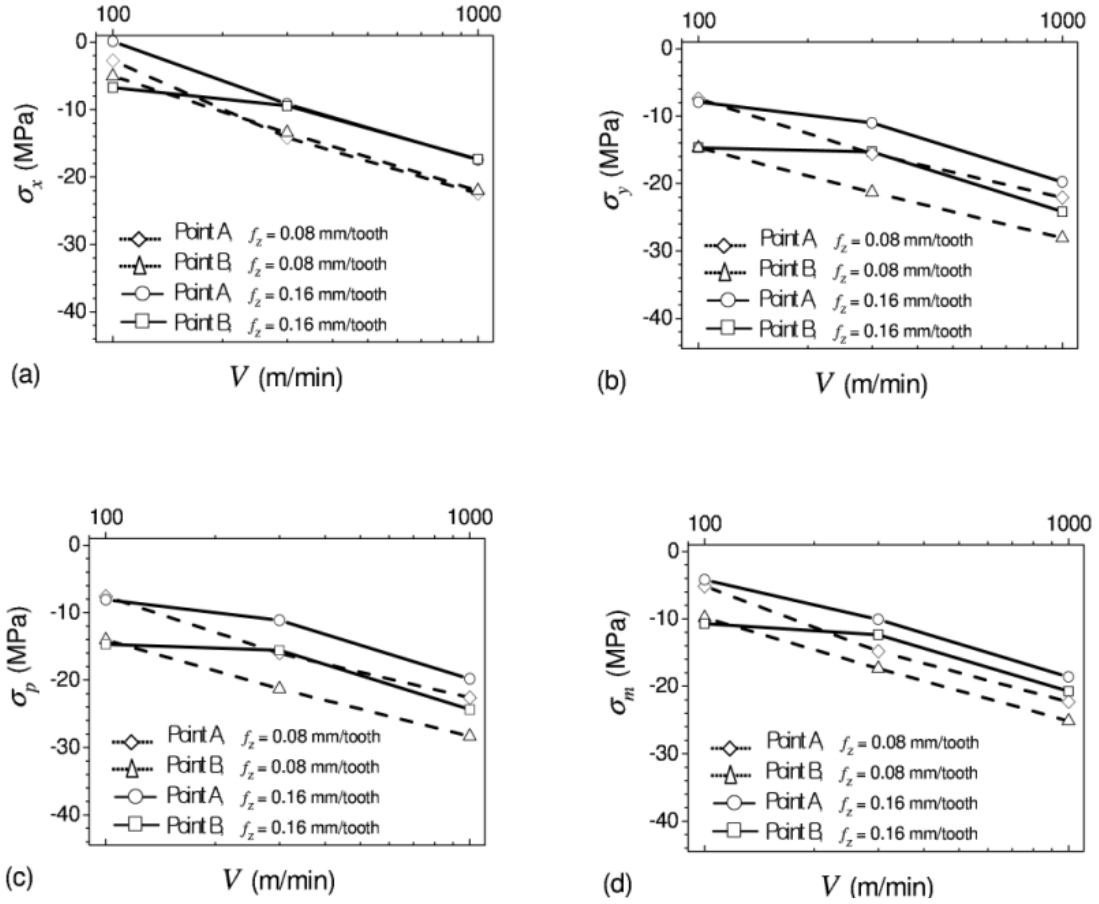

Fig. 3: Residual stress components (a) σ_x, (b) σ_y, (c) σ_p and (d) σ_m in function of cutting speed (d = 0.4 mm)

evaluated feed rate. Therefore, it is possible to affirm that, for the lower cutting speed, in each centroid the tool generates the same plastic stretching for both feed rates. In contrast, for the medium and high cutting speeds, the higher feed rate would adapt better to the cutting operation resulting in low plastic stretching and as a consequence, in lower residual stress values.

Figure 3c shows the normal component σ_p which is associated to a principal direction. It must be noted that principal directions are those where normal components reach their maximum and minimum (Gere, 2001). In this case σ_p corresponds to the more compressive normal component. The results for this component are very similar to those corresponding to the σ_y component. Therefore, the principal direction associated with σ_p will be very close to the y direction. It is very important to note that the latter is the direction of the feed rate and also the rolling direction of the evaluated material.

Figure 3d shows the σ_m component, which corresponds to the mean value of the principal components. A significant fact is that, as it occurs with the σ_y and σ_p components, for the lower cutting speed each centroid has its stress value which is independent of the evaluated feed rate ─in each centroid, the plastic stretching would be the same for the different feed rates. Moreover, between V = 300 m/min and V = 1000 m/min, the segments are equi-spaced and parallel. In addition, the stress range is narrow, which is similar to the case of the σ_x component. Also, unlike σ_y and σ_p the functions associated to each feed rate are not overlapped.

Figure 4 shows Mohr's circles corresponding to the centroid A. It is important to note that the coordinates of each point of each circle represent the residual stress components corresponding to an infinitesimal element, which is rotated an angle θ with respect to the reference axes x and y (Gere, 2001). Therefore, each circle has the particularity of showing the different states of residual stress for each of possible directions. Furthermore, the small segment showing each circle correspond to the reference direction (θ = 0 in Fig. 2). These circles show different diameters which mean different levels of anisotropy. Moreover, these circles are independent. The circle associated to the higher cutting speed represents to the residual stress state more isotropic and compressive. It should be noted that the medium component of residual stress corresponds to the abscissa value which is located at the circle center. Regarding the directions associated with the more

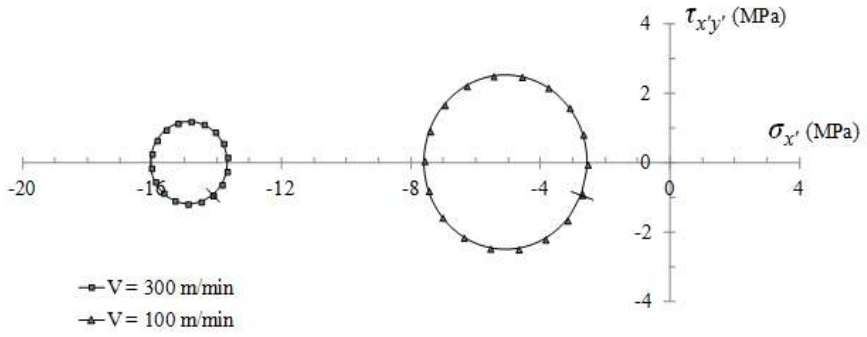

Fig. 4: Mohr's circles corresponding to the centroid A (f_z = 0.08 mm/tooth, d = 0.4 mm)

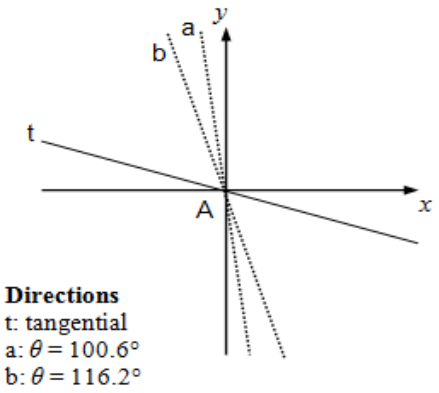

Fig. 5: Directions corresponding to the component σ_p (centroid A, f_z = 0.08 mm/tooth; d = 0.4 mm; a: V = 100 m/min y b: V = 300 m/min)

Table 4: Medium stress difference between the centroids A and B

Cutting speed V (m/min)	Medium stress difference $\Delta\sigma_m$ (MPa)	
	f_z = 0.08 mm/tooth	f_z = 0.16 mm/tooth
100	4.68	6.51
300	2.55	2.29
1000	2.85	2.15

compressive residual stress, Fig. 5 shows such directions. In this figure, the coordinate origin corresponds to the centroid A. It is important to mention that the analysis does not include the direction associated to V = 1000 m/min because its high anisotropy level increases the error of localization of direction. Figure 5 shows that both directions are between the y direction ─material rolling direction─ and cutting tangential direction. The angular difference between these directions is 63.6°. It is noteworthy that these results corroborate those obtained from other cutting conditions, where the behaviour of two different types of aluminium alloys were compared (Díaz *et al*., 2012). From both studies it is inferred the important role played by the rolling direction of the original material in the generated residual stress states.

The analysis of the medium component of residual stress is independent of the anisotropy level revealed by the Mohr's circles. This is because the abscissa of this medium component corresponds to circle center. In turn, it is important to note that this component is associated to two directions, in which the tangential components are maximum in absolute value. Table 4 shows the medium component difference between the centroids A and B. It is noteworthy that this difference is always positive, which means that the stress values at the centroid B are more compressive than at the centroid A for all cases. Through the analysis of this table, it is possible to advert that for each cutting speed the difference between both values it is not significant. Therefore, the medium component difference is independent of the feed rate. The highest increases were obtained for the lower cutting speed. This fact implicates larger difference of plastic stretching between both centroids, which would be due to a great difference in the adaptation of the cutting edge for both zones.

In addition, it is possible to affirm that the change of the residual stress medium component is independent of the cutting speed for the cases of medium and high speed. Therefore, the plastic stretching difference between both centroids would be very similar for various combinations of feed rate and cutting speed. Finally, this fact implies similar differences in the combination between local plastic deformation amount (mechanical effect) and heat conducted to the new surface (thermal effect) between both centroids. This phenomenon is only possible for those directions associated to the medium normal component, besides those directions present the maximum tangential stresses for each of the evaluated process parameters combinations.

CONCLUSION

The micro-indent method used in this study enabled to determine different components of residual stress, which were generated via face milling in samples of AA 7075-T6 aluminium alloy. These components were determined at different zones of the new surface. These zones show asymmetries due to differences in cutting edge orientation. The symmetries

obtained for the σ_x component and the asymmetries obtained for the σ_y component were explained based on the connection between the cutting speed components and feed rate. The direction associated to the more compressive principal component is very close to the rolling direction of the studied material. This observable fact shows the importance of this process in the obtained residual stress states. Finally, the analysis of the medium normal component allowed detecting that the plastic stretching difference between both evaluated zones is very similar for different combinations of cutting speed and feed rate. This fact implies that, the difference in the combination of local plastic damage and heat amount conducted to the new surface, between both studied zones, remains unchanged for different combinations of process parameters.

ACKOWLEDGMENT

The authors acknowledge the financial support of Universidad Tecnológica Nacional and Consejo Nacional de Investigaciones Científicas y Técnicas of Argentina.

NOMENCLATURE

A	:	Elongation (%)
d	:	Depth of cut (mm)
E	:	Longitudinal elastic modulus (GPa)
f_z	:	Feed per tooth (mm/tooth)
HV0.5	:	Vickers micro-hardness (test load: 500 gf)
V	:	Cutting speed (m/min)
V_x	:	Cutting speed component at the x direction (MPa)
V_y	:	Cutting speed component at the y direction (MPa)
v_f	:	Table feed (m/min)
ε_x	:	Deformation component at the x direction
ε_y	:	Deformation component at the y direction
θ	:	Angle formed by an arbitrary direction and the axis $y = 0$
υ	:	Poisson's ratio
σ_m	:	Medium component of residual stress (MPa)
σ_p	:	More compressive principal component of residual stress (MPa)
σ_x	:	Residual stress component at the x direction (MPa)
$\sigma_{x'}$	:	Normal stress component associated to an angle θ (MPa)
σ_y	:	Residual stress component at the y direction (MPa)
σ_u	:	Ultimate tensile strength (UTS) (MPa)
$\sigma_{y_{02}}$	:	Yield strength (MPa)
τ_{xy}	:	Tangential stress component (MPa)
$\tau_{x'y'}$	:	Tangential stress component associated to an angle θ (MPa)
$\Delta\sigma_m$	:	Medium stress difference (MPa)

REFERENCES

Abrão, A.M., J. Silva Ribeiro and J. Paulo Davim, 2011. Surface Integrity. In: Paulo Davim, J. (Ed.), Machining of Hard Materials. Springer-Verlag, London, pp: 115-141.

Brinksmeier, E., 1987. Residual stresses in hard metal cutting. Residual Stresses Sci. Technol., 2: 839-847.

Brinksmeier, E., J.T. Cammett, W. König, P. Leskovar, J. Peters and H.K. Tönshoff, 1982. Residual stresses-measurement and causes in machining processes. Ann. CIRP, 31: 491-510.

Capello, E., 2005. Residual stresses in turning. Part I: Influence of process parameters. J. Mater. Process. Tech., 160: 221-228.

Curtis, M.A. and F.T. Farago, 1994. Handbook of Dimensional Measurement. Industrial Press Inc., New York.

Díaz, F.V. and C. Mammana, 2012. Study of Residual Stresses in Conventional and High-speed Milling. In: Filipovic, L. (Ed.), Milling: Operations, Applications and Industrial Effects. Nova Science Publishers Inc., New York, pp: 127-155.

Díaz, F.V., R. Bolmaro, A. Guidobono and E. Girini, 2010. Determination of residual stresses in high speed milled aluminium alloys using a method of indent pairs. Exp. Mech., 50: 205-215.

Díaz, F.V., C. Mammana and A. Guidobono, 2012. Evaluation of residual stresses induced by high speed milling using an indentation method. Modern Mech. Eng., 2: 143-150.

Dotson, C.L., R. Harlow and R. Thompson, 2003. Fundamentals of Dimensional Metrology. 5th Edn., Thompson Delmar Learning, New York.

Fuh, K.H. and C. Wu, 1995. A residual stress model for the milling of aluminium alloy (2014-T6). J. Mater. Process. Tech., 51: 87-105.

Gere, J.M., 2001. Mechanics of Materials. 5th Edn., Brooks/Cole, Pacific Grove, CA.

Henriksen, E.K., 1951. Residual stress in machined surfaces. Trans. ASME, 73: 265-278.

Jacobus, K., S.G. Kapoor and R.E. DeVor, 2001. Experimentation on the residual stresses generated by endmilling. J. Manuf. Sci. E-T. ASME, 123: 748-753.

Mammana, C.A., F. Díaz, A. Guidobono and R. Bolmaro, 2010. Study of residual stress tensors in high-speed milled specimens of aluminium alloys using a method of indent pairs. Res. J. Appl. Sci. Eng. Technol., 2: 749-756.

Mao, W., 2003. Recrystallization and Grain Growth. In: Totten, G.E. and D. MacKenzie, (Eds.), Handbook of Aluminum. Physical Metallurgy and Processes. Marcel Dekker Inc., New York, 1: 211-258.

Özel, T. and E. Zeren, 2004. Determination of flow material stress and friction for FEA of machining using orthogonal cutting tests. J. Mater. Process. Tech., 153: 1019-1025.

Schwach, D.W. and Y. Guo, 2006. A fundamental study on the impact of surface integrity by hard turning on rolling contact fatigue. Int. J. Fatigue, 28: 1838-1844.

Withers, P.J., 2007. Residual stress and its role in failure. Rep. Prog. Phys., 70: 2211-2264.

Wyatt, J.E. and J. Berry, 2006. A new technique for the determination of superficial residual stresses associated with machining and other manufacturing processes. J. Mater. Process. Tech., 171: 132-140.